

Upscaling hydraulic conductivity: theory and examples from geohydrological studies

M.F.P. Bierkens & J.W.J. van der Gaast

The Winand Staring Centre for Integrated Land, Soil and Water Research (SC-DLO) P.O. Box 125, 6700 AC, Wageningen, The Netherlands

Key words: groundwater flow, upscaling, heterogeneity, stochastic, confining layers

Abstract

This paper presents an overview of the theory of upscaling hydraulic conductivity and describes two case studies in which some of this theory has been applied. The representative hydraulic conductivity of a numerical model block ('block conductivity' for short) is defined in terms of smaller scale hydraulic conductivities. Also, using elementary examples, some general properties of block conductivities are given. Analytical solutions for the block conductivity are presented that were derived by various authors for uniform flow conditions both in a deterministic and in a stochastic setting. Some results of the hydraulic upscaling theory are illustrated by two case studies from the Netherlands. The first case study deals with deriving the representative hydraulic conductivity tensor of a clay layer. Upscaling results are compared with traditional harmonic averaging. In the second case study the upscaling is used to derive the three-dimensional distribution of block conductivities for a numerical groundwater model of a confining layer of complex deposits. Here stochastic upscaling is used together with a geostatistical simulation approach. The simulated block conductivities are used in a numerical groundwater model and results are compared with pumping tests. When the upscaling is ignored groundwater flow through the deposits is predicted wrongly.

Introduction

In geohydrological studies that involve complex environmental questions scale inconsistency is very common. The scale at which transport and flow phenomena in the porous media are best described is usually very different from (i.e. larger than) the scale at which measurements are available, but also very different from (i.e. smaller than) the scale required for management decisions. When focusing at the modelling of groundwater flow and transport the following spatial scales are often distinguished [2,8]:

- 1) the *pore scale* (10^{-6} – 10^{-2} m); the scale at which flow and transport through porous media is described in terms of forces and mass fluxes within the fluid phase and the solid phase and between these phases. Groundwater flow for instance is described by the Navier-Stokes equations.
- 2) the *core scale* (10^{-1} – 10^0 m); the scale at which flow and transport are described in terms of continuity equations and simplified flux equations such as Darcy's law and Fick's law. The minimum scale

at which these simplified flux equations are valid is called the representative elementary volume (REV) [1]. This is exactly the scale at which measurements of hydraulic properties are performed on samples from drilling cores;

- 3) the *model block scale* (10^1 – 10^2 m); the scale of blocks or elements of numerical flow and transport models;
- 4) the *local scale* (10^2 – 10^3 m); the scale at which groundwater flow and -transport is considered as three-dimensional. Examples of local scale groundwater problems are pollution and remediation studies around waste sites and the assessment of travel time distributions in protection areas around drinking water wells;
- 5) the *regional scale* (horizontal dimension 10^3 – 10^5 m); the scale at which the subsoil is divided into permeable layers (aquifers) and less permeable layers (aquitards). The groundwater flow through aquifers is considered to be mainly horizontal and the flow through the aquitards mainly vertical. The lowering of water tables due to groundwa-

ter abstraction is often modelled at this scale. The assumption that the flow in aquifers is predominantly horizontal is valid when the horizontal extent of the model domain is much larger than the vertical extent. This is usually the case for large model areas (horizontal 10^3 - 10^5 m) in alluvial and marine deposits (vertical extent of the model domain 10^2 m).

It is possible to derive the simplified flux equations that are valid at the core scale from the differential equations that are valid at the pore scale. This amounts to spatial averaging [38] or statistical averaging [8] of the pore scale differential equations. Then a so called ‘closure problem’ is solved to arrive at simplified flux equations with representative parameters such as hydraulic conductivity and dispersivity that are valid at the core scale. The pore scale processes are thus captured by the representative parameters; i.e. the hydraulic conductivity in Darcy’s law and the groundwater flow equation and the dispersivity in Fick’s law and the convection-dispersion equation. Such representative parameters are also encountered in soil physics: the soil water retention curve and unsaturated conductivity curve in Richards’ equation.

The pore scale is usually not considered in practical groundwater modelling studies. Instead, one directly starts with the simplified core scale equations and the representative parameters are measured directly on sediment cores. These equations are then used to describe local scale and regional scale groundwater problems. However, hydraulic properties such as hydraulic conductivity and dispersivity that are measured on sediment cores cannot be used to describe flow and transport at larger scales. The reason for this is that hydraulic properties usually exhibit a large spatial heterogeneity [34]. Often this is not a serious problem for regional scale problems. Modified two-dimensional equations can be readily derived for these scales [14]. Representative hydraulic properties for this scale, such as transmissivities, can be derived from large scale pumping tests. Of course one still has to deal with regional scale spatial heterogeneities but this rarely involves scale transformations.

The real scale conflicts are encountered in local scale groundwater problems, which are the focus of this paper. To model the three-dimensional groundwater flow through heterogeneous media a numerical groundwater model is required. The discretization into blocks or elements that is required for numerical modelling cannot be done at the core scale, because this would result in a numerical model that is far

beyond the capacity of the current computers. Thus, the blocks or elements of numerical groundwater models are generally much larger than the size of the core scale elements (horizontal extent 100–1000 m). Apart from inverse modelling procedures [6,25] there are few measurement techniques that yield directly representative hydraulic properties for these model blocks (the spatial extent of pumping tests is too large). Instead, they need to be derived from measurements at the core scale, i.e. from column experiments by means of scale transformations. This derivation of representative hydraulic properties for a larger scale from smaller scale hydraulic properties is called ‘upscaling’.

This paper only deals with the upscaling of saturated hydraulic conductivity. For local scale groundwater problems the upscaling problem is then defined as: ‘Given that measurements of hydraulic conductivity are available at the core scale, derive representative hydraulic conductivities (block conductivities) for the numerical model blocks’. The paper serves two goals: 1) to present a brief review of the upscaling theory that has been used in geohydrology to obtain block conductivities; 2) to illustrate the application of upscaling theory by means of two cases studies.

The remainder of this paper is set up as follows: First the block conductivity is defined in mathematical terms and its properties are discussed. Next, some theoretical results for uniform flow are presented in a deterministic and stochastic context. Finally, two case studies are described where some of the upscaling theory has been applied.

The theory of upscaling hydraulic conductivity

Definition of block conductivity

The block conductivity can be defined in several manners. For instance, it can be derived as a representative conductivity that arrives from volume averaging of the groundwater flow equations, much in the same manner as the core scale hydraulic conductivity is derived from the pore scale equations. Usually, the block conductivity $\mathbf{K}_b(\mathbf{x}')$ is defined as the conductivity that relates the average flux through a block of size V (with centre point \mathbf{x}') to the mean head gradient within the block [30]:

$$(1/V) \int_V \mathbf{q}(\mathbf{x}) d\mathbf{x} = -\mathbf{K}_b(\mathbf{x}') (1/V) \int_V \nabla \mathbf{h}(\mathbf{x}) d\mathbf{x} \quad (1)$$

with $\mathbf{q}(\mathbf{x})$ and $\nabla \mathbf{h}(\mathbf{x})$ are the flux and hydraulic head gradient at the measurement scale respectively. A bold

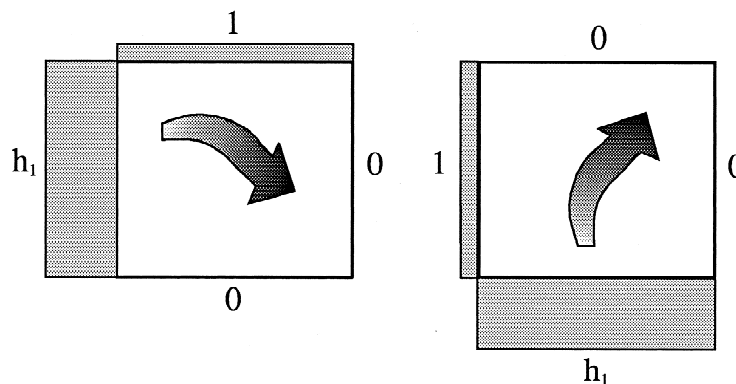


Figure 1. Boundary conditions used to calculate the block conductivity with equations (2).

face notation is used for the vectors \mathbf{x} , $\mathbf{q}(\mathbf{x})$ and $\nabla\mathbf{h}(\mathbf{x})$. If $\mathbf{K}_b(\mathbf{x})$ is unique and it exists it is called the block conductivity tensor.

Some properties of the block conductivity

The block conductivity as previously defined has a number of general properties.

- 1) The block conductivity is not equal to the arithmetic average of the core scale conductivities. This is immediately clear when one considers vertical flow in a horizontally layered medium. The representative conductivity then equals the harmonic average (Eq. 7) of the layers and not the arithmetic average.
- 2) The block conductivity is dependent on the flow geometry. To demonstrate this, a simple numerical example is given: Consider the two-dimensional flow through a block that is made up of 64 (8×8) scalar conductivities. To calculate the four elements of the block conductivity tensor of the larger block we need two sets of (equivalent) boundary conditions (see Fig. 1). Using a numerical groundwater model we can calculate for each of the sets of boundary conditions of Figure 1: 1) the block averaged fluxes in the x - and y -directions, $\langle q_x \rangle$ and $\langle q_y \rangle$; 2) the block averaged hydraulic gradients in the x - and y -directions, $\langle \Delta h / \Delta x \rangle$ and $\langle \Delta h / \Delta y \rangle$. The brackets $\langle \rangle$ represent the block average. For each set of boundary conditions we can express Darcy's law at the block scale:

$$\langle q_x \rangle^1 = -K_{Bxx} \langle \Delta h / \Delta x \rangle^1 - K_{Bxy} \langle \Delta h / \Delta y \rangle^1 \quad (2a)$$

$$\langle q_y \rangle^1 = -K_{Byx} \langle \Delta h / \Delta x \rangle^1 - K_{Byy} \langle \Delta h / \Delta y \rangle^1 \quad (2b)$$

$$\langle q_x \rangle^2 = -K_{Bxx} \langle \Delta h / \Delta x \rangle^2 - K_{Bxy} \langle \Delta h / \Delta y \rangle^2 \quad (2c)$$

$$\langle q_y \rangle^2 = -K_{Byx} \langle \Delta h / \Delta x \rangle^2 - K_{Byy} \langle \Delta h / \Delta y \rangle^2 \quad (2d)$$

The superscripts 1,2 stand for the first and second set of boundary conditions respectively. From these equations the four unknown elements of the block conductivity tensor K_{Bij} ($i, j = xy$) can be uniquely solved. This procedure can be repeated for different values of h_1 in Figure 1, thereby changing the boundary conditions around the blocks. The results are shown in Figure 2. Clearly, the elements of the block conductivity tensor change with the boundary conditions. This may have serious repercussions for inverse modelling. Suppose that block conductivities are obtained from calibration of a groundwater model to head measurements under natural flow conditions. These block conductivities are not necessarily suitable to predict the effects of for instance pumping wells where the flow geometry is very different. This may limit the predictive power of calibrated groundwater models.

From the numerical experiment of Figure 1 two additional properties of block conductivity can be derived:

- 3) The block conductivity can be a tensor even if the core scale conductivities are scalars.
- 4) The block conductivity tensor is not necessarily symmetric, even if the conductivity tensor at the measurement scale is symmetric or a scalar. This was shown in a more rigorous manner by Zijl and Stam [40].

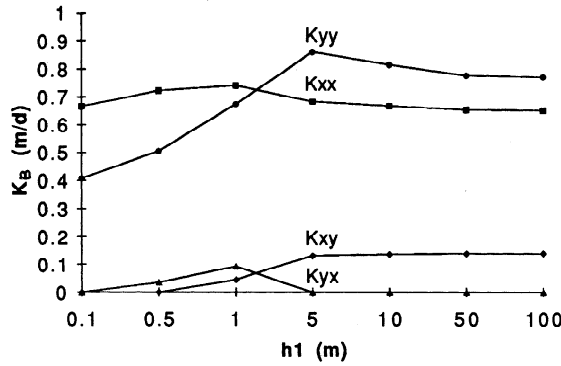


Figure 2. Relation between the components of the block conductivity tensor and the value of h_1 .

The dependence of the block conductivity to boundary conditions can be shown in a more rigorous manner. For this we express the variables $\mathbf{q}(\mathbf{x})$, $\nabla\mathbf{h}(\mathbf{x})$ and $\mathbf{k}(\mathbf{x})$ in Darcy's law as a perturbation around their block averages: $\mathbf{q}(\mathbf{x}) = \langle\mathbf{q}\rangle + \mathbf{q}'(\mathbf{x})$, $\nabla\mathbf{h}(\mathbf{x}) = \langle\nabla\mathbf{h}\rangle + \nabla\mathbf{h}'(\mathbf{x})$ and $\mathbf{k}(\mathbf{x}) = \langle\mathbf{k}\rangle + \mathbf{k}'(\mathbf{x})$, where $\langle\mathbf{q}\rangle$, $\langle\nabla\mathbf{h}\rangle$ and $\langle\mathbf{k}\rangle$ are the block averages and $\mathbf{q}'(\mathbf{x})$, $\nabla\mathbf{h}'(\mathbf{x})$ and $\mathbf{k}'(\mathbf{x})$ the deviations around this block average within the block. Substitution in Darcy's law and averaging both sides for the block gives

$$\langle\langle\mathbf{q}\rangle + \mathbf{q}'(\mathbf{x})\rangle = \langle - (\langle\mathbf{k}\rangle + \mathbf{k}'(\mathbf{x})) (\langle\nabla\mathbf{h}\rangle + \nabla\mathbf{h}'(\mathbf{x})) \rangle \quad (3)$$

Expanding equation (3) and using $\langle\mathbf{q}'(\mathbf{x})\rangle = \langle\nabla\mathbf{h}'(\mathbf{x})\rangle = \langle\mathbf{k}'(\mathbf{x})\rangle = 0$ gives

$$\langle\mathbf{q}\rangle = -\langle\mathbf{k}\rangle\langle\nabla\mathbf{h}\rangle - \langle\mathbf{k}'(\mathbf{x})\nabla\mathbf{h}'(\mathbf{x})\rangle \quad (4)$$

We can see that the block averaged Darcy's law is made up of a term consisting of block averages and a closure term. This closure term essentially accounts for the block-averaged covariation of $\nabla\mathbf{h}(\mathbf{x})$ and $\mathbf{k}(\mathbf{x})$. If we want to write (4) in the same form as the original Darcy's law it is necessary to assume that the closure term has the following form: $\langle\mathbf{k}'(\mathbf{x})\nabla\mathbf{h}'(\mathbf{x})\rangle \equiv \mathbf{K}'\langle\nabla\mathbf{h}\rangle$, where \mathbf{K}' is some kind of block-effective conductivity accounting for the deviations from the average. It follows that

$$\langle\mathbf{q}\rangle = -(\langle\mathbf{k}\rangle + \mathbf{K}')\langle\nabla\mathbf{h}\rangle = -\mathbf{K}_b\langle\nabla\mathbf{h}\rangle \quad (5)$$

Equation (5) is Darcy's Law defined at the block scale with \mathbf{K}_b the block conductivity. However from equations (4) and (5) we can see that for \mathbf{K}_b the following relation holds:

$$\mathbf{K}_b\langle\nabla\mathbf{h}\rangle = \langle\mathbf{k}\rangle\langle\nabla\mathbf{h}\rangle + \langle\mathbf{k}'(\mathbf{x})\nabla\mathbf{h}'(\mathbf{x})\rangle \quad (6)$$

It is obvious from equation (6) that \mathbf{K}_b is still dependent on the closure term $\langle\mathbf{k}'(\mathbf{x})\nabla\mathbf{h}'(\mathbf{x})\rangle$ which is dependent on the solution at the core scale. As the solution at the core scale is dependent on the boundary conditions around the block (i.e. the flow geometry) so is the block conductivity.

Direct and indirect upscaling methods

Upscaling methods that derive block conductivities from Darcy's law can be divided into indirect or deterministic upscaling methods and direct or stochastic upscaling methods. When indirect upscaling is used the conductivity field within the block must first be defined at a smaller scale, either by deterministic mapping or by stochastic simulation. Next, the upscaling is performed to obtain the conductivity tensors for the model blocks. The scale transformation is a deterministic averaging procedure of the mapped or simulated conductivities within the block, for instance taking the geometric average (Eq. 8) in two dimensions. Therefore, indirect upscaling methods are also referred to as deterministic. With direct upscaling methods first the spatial probability distribution statistics of the block conductivity tensors are derived from the statistical properties of the smaller scale conductivities, which are assumed to constitute a random field. Next, the block conductivities are generated directly by stochastic simulation from the derived probability distribution. Because the scale transformation involves scaling up of probability distributions, direct upscaling methods are termed stochastic.

Some theoretical results from deterministic upscaling

If we assume that 1) the flow through the block is more or less uniform (i.e. slowly varying non-diverging flow lines) and 2) the core scale conductivities are isotropic (at one point in space the core scale conductivity has the same value in all directions, i.e. it is a scalar) then the block conductivity is a scalar and is given by ($K_b(\mathbf{x}')$ is the block conductivity for a block V with centre point \mathbf{x}' and $k(\mathbf{x})$ the core scale conductivity):

- 1) for one-dimensional flow: the harmonic block average [9]:

$$K_b(\mathbf{x}') = \left\{ (1/V) \int_V [k(\mathbf{x})]^{-1} d\mathbf{x} \right\}^{-1} \quad (7)$$

- 2) for two-dimensional flow and square blocks: the geometric block average [10]:

$$K_b(\mathbf{x}') = \exp\left\{ (1/V) \int_V \ln[k(\mathbf{x})] d\mathbf{x} \right\} \quad (8)$$

3) for three-dimensional flow and cubic blocks: up to recently no analytical results were available for this case. Desbarats [11] found by means of a simulation study the following result that is consistent with results from stochastic theory [17]:

$$K_b(\mathbf{x}') = \left\{ (1/V) \int_V [k(\mathbf{x})]^{1/3} d\mathbf{x} \right\}^3 \quad (9)$$

Recently Sánchez-Vila et al. [32] have derived this result analytically.

Deterministic upscaling methods that are valid for anisotropic media and non-cubic blocks are, among others, given by Kasap and Lake [23] and Desbarats [11] for uniform flow and by King [24], Desbarats [12], Zijl and Stam [40] and Bierkens and Weerts [4] for various other flow geometries. Kasap and Lake [23] present analytical results, Desbarats [11,12] heuristic power averaging methods and King [24] and Bierkens and Weerts [4] a numerical upscaling procedure. The only analytical solutions for non-uniform flow that are not non-local (i.e. involve no integration outside the model block) are given by Zijl and Stam [40]. However, these solutions are only valid for thin blocks and (imperfectly) layered anisotropic media where the layering is parallel to the block sides. Moreover, to apply these solutions the boundary fluxes and heads of the model blocks must be known, which means the core scale problem must be solved. This makes the practical application of their method problematic, because the reason that upscaling is necessary in the first place is that numerical models at the core scale cannot be solved even with the largest computers.

Some theoretical results from stochastic upscaling

When stochastic upscaling methods are used to derive block conductivities the heterogeneous spatial variation of core scale conductivities is usually modelled as a random field. Because the natural logarithm of the core scale conductivity $\ln[\mathbf{k}]$ is often found to be Gaussian distributed [15], one usually models the logconductivity $\mathbf{y}(\mathbf{x}) = \ln[\mathbf{k}(\mathbf{x})]$ as a stationary multivariate Gaussian random field $\mathbf{Y}(\mathbf{x})$, which can then be described with the mean $E[\mathbf{Y}(\mathbf{x})]$ ($E[\cdot]$ stands for mathematical expectation) and the covariance function $C_{\mathbf{Y}}(\mathbf{h})$, where \mathbf{x} is a space vector and \mathbf{h} is a separation vector between two locations in space. Naturally, because the core scale hydraulic conductivities are stochastic, so are the block conductivities.

Analytical solutions of the stochastic block conductivity are available given the following conditions: 1) the core scale logconductivities are scalar fields $y(\mathbf{x}) =$

$\ln[k(\mathbf{x})]$ (i.e. isotropic core scale conductivities); 2) the core scale logconductivity is modelled as a stationary multiGaussian random field $Y(\mathbf{x})$ with geometric mean $K_g = \exp(E[\ln(K)])$ and variance σ_Y^2 ; 3) the random field $Y(\mathbf{x})$ is statistically isotropic (i.e. the covariance function of core scale logconductivity is the same in all directions); 4) the flow field is statistically uniform (i.e. $E[\nabla \mathbf{h}(\mathbf{x})] = E[\nabla \mathbf{h}] = \text{constant}$) or is at least slowly varying compared to the size of the flow domain; 5) the block size is very large compared to the correlation length of the core scale logconductivity; the correlation length is the distance over which the random field variables at two different locations remain correlated. Due to the last condition one can argue that the variances of the block conductivities are almost zero. So the block conductivities become deterministic constants that are equal to the medium effective conductivity (the representative conductivity of the entire porous medium). Conditions 1) and 3) entail that these constants are scalars and conditions 2) and 4) that they are the same for every block in the flow domain:

1) one-dimensional flow [27]:

$$K_b(\mathbf{x}') = K_g \exp(-\sigma_Y^2/2) \quad (10)$$

2) two-dimensional flow [7,27]:

$$K_b(\mathbf{x}') = K_g \quad (11)$$

3) three-dimensional flow and assuming that σ_y^2 is not too large ($\sigma_y^2 \ll 1$) [17]:

$$K_b(\mathbf{x}') = K_g \exp(1 + \sigma_Y^2/6) \quad (12)$$

Equation (11) can be useful in regional scale model studies. If for an aquifer a number of transmissivities are known from pumping tests and the model blocks are very large compared to the correlation length, but small enough to have approximately uniform flow through them equation (11) can be readily used. The block conductivity can be estimated by taking the geometric average of the transmissivities obtained from pumping tests. Equation (12) is not much use for three-dimensional modelling because most sediments show sedimentary layering so that statistical isotropy is not likely to occur.

If the block sizes are not large compared to the correlation length, the block conductivities are stochastic and constitute a random field. Several researchers derived analytical solutions for the expected value $E[Y_b(\mathbf{x})]$, the variance $\sigma_{Y_b}^2$ and/or the covariance $C_{Y_b}(\mathbf{h})$ for the random field $Y_b(\mathbf{x}) = \ln[K_b(\mathbf{x})]$ subject to above conditions 1) to 4). Indelman [18] shows

that $Y_b(\mathbf{x})$ is approximately Gaussian distributed. If we also assume multiGaussianity for $Y_b(\mathbf{x})$ these upscaled statistics are thus sufficient to generate block conductivity fields by means of stochastic simulation. For statistically isotropic media and square blocks the analytical results of Rubin and Gómez-Hernández [30] and Desbarats [10] can be used. For statistically anisotropic media and blocks of arbitrary form the results of Indelman and Dagan [19,20] are available. Their method was used in the case studies shown later. A rigorous comparison of the aforementioned stochastic upscaling methods is given by Sánchez-Vila et al. [32].

For non-uniform flow conditions no analytical solutions for the statistics of the block conductivities are available. Bierkens [2] showed that the uniform flow solution (11) gave satisfactory results for highly non-uniform flow in two dimensions, even for blocks that were only slightly larger than the integral scale of core scale conductivities. Results were even better when taking exponentials of block estimates that were obtained from block-kriging logconductivities from a limited number of measurement points. It must be stressed that these are only heuristic approaches and should be used with care. Also, block-kriging of logconductivities can only be used when the observations are on a regular grid such that no differences in smoothness of the block conductivity field occur.

Case studies

To illustrate the use of upscaling techniques in practice, two case studies are presented. The first case study [36] involves a straight forward application of the upscaling theory of Indelman and Dagan [19,20]. In the second case study [2] the upscaling theory of Indelman and Dagan [19,20] is applied to characterize the conductivity spatial structure of highly complex deposits.

Case 1: Geohydrological research Purmerbos

The goal of the research that is described in this case study was to characterize the geohydrological structure of the confining layer of the Purmerbos forrest area. A confining layer is a set of (often horizontally layered) Holocene deposits that cover most of the aquifers in the marine and fluvial district of the Netherlands. They protect the groundwater in the aquifers from pollution from the surface. The geohydrology of the confining layer of the Purmerbos forrest area had to be deter-

mined as part of a water balance study of this area [36].

The confining layer of the Purmerbos area has a rather simple architecture. It consists of three distinct sublayers. A clay and peat layer at the bottom, a sandy layer in the middle and a clay layer at the top. One expects the flow through the top and bottom sublayers to be mainly vertical, while the flow through the sandy layer in between may be horizontal, for instance near water courses. The vertical resistance to flow is usually expressed in terms of a C-value [T] which is the thickness of the layer divided by its vertical hydraulic conductivity. The horizontal flow conductance is expressed in terms of the transmissivity [L^2T^{-1}], which is the product of the horizontal conductivity and the layer thickness. Using pumping tests [26], the transmissivity of the sandy sublayer and the aquifer were determined as well as the C-value of the lower sublayer.

The C-value of the upper sublayer could not be derived from pumping tests. It should have been derived from the pumping test that was performed to obtain the transmissivity of the middle sublayer. However, the duration of this test was too short to properly estimate this C-value. Therefore, to obtain an estimate of this C-value sets of three undisturbed samples were taken at randomly selected depths of 21 drillings whose coordinates were also selected at random. This resulted in a total of 63 samples (sample length 30 cm, sample diameter 5.7 cm). Hydraulic conductivities of the samples were measured using a permeameter specifically designed to measure saturated conductivity on sediment cores [39]. To arrive at a C-value for the entire upper sublayer we need the average thickness of this layer as well as the representative vertical hydraulic conductivity of this layer. This means that we are faced with an upscaling problem: Given that measurements are taken at the core scale, what is a representative vertical hydraulic conductivity for the entire upper sublayer. Two methods were used. A traditional method and the upscaling method of Indelman and Dagan [19,20].

Traditional averaging

The traditional way of deriving the C-value from samples is to first derive a C-value for each drilling by means of harmonic averaging of the conductivities of this drilling and then to calculate the C-value of the entire layer by harmonic averaging of the C-values of all drillings. These averaging rules, which assume the

flow through the layer to be strictly vertical, are directly derived from the analogy of resistor networks in electricity. The C-value at a drilling site is thus obtained as:

$$C_i = \frac{d_i}{m_i} \sum_{j=1}^{m_i} \frac{1}{k_{ij}} \quad (13)$$

where k_{ij} is the measured vertical conductivity of the j th sample in i th drilling, d_i is the thickness of the layer at drilling i , C_i the resulting c-value and m_i the number of samples in drilling i (here $m_i = 3$). Next the C-value of the entire layer follows from:

$$C = \left[\frac{1}{n} \sum_{i=1}^n \frac{1}{C_i} \right]^{-1} \quad (14)$$

with n the number of drillings ($n=21$). The result of this averaging procedure is a representative C-value of the upper clay layer of 973 days.

Stochastic upscaling

The upscaling method of Indelman and Dagan [19,20] assumes that the flow through the layer is statistically uniform; i.e. the average flow is uniform. The average uniform flow does not have to vertical but can cross the layer at any angle. Furthermore, the method not only yields a vertical representative conductivity of the layer but also a horizontal representative conductivity. Also, because it is a stochastic upscaling method it not only estimates the block conductivities but also their confidence limits. The core scale logconductivity $y = \ln[k]$ is assumed scalar and modelled as a stationary multivariate Gaussian random field $Y(\mathbf{x})$. The spatial covariance can be anisotropic. It is assumed that the principal directions of anisotropy are aligned with the coordinate system. This random field is characterized by the following parameters:

- geometric mean: $K_g = \exp(E[\ln(k)])$,
- variance σ_Y^2 of the logconductivity,
- integral scales. Like the correlation length, the integral scales are correlation measures in the principal directions of anisotropy. The larger the integral scale the larger the distance over which logconductivities remain spatially correlated in that direction. We assumed that the integral scales in all horizontal directions are the same and larger than the integral scale in the vertical direction. We therefore need only two integral scales:

I_{Y_h} : the horizontal integral scale,

I_{Y_v} : the vertical integral scale.

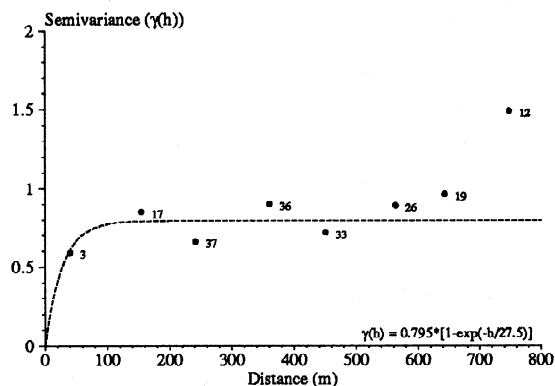
From the histogram of logconductivities it was derived that $K_g = 0.00329$ m/d and $\sigma_Y^2 = 0.869$. To determine the integral scales the semivariograms of logconductivity in the horizontal and vertical direction were estimated from the data [21]. Next, the exponential variogram model $\gamma(\mathbf{h}) = a(1 - \exp[-\mathbf{h}/I])$ was fitted to the experimental semivariograms. The fitted parameters I were then taken as estimates of the integral scales [2]. This resulted in a horizontal integral scale of 27.5 m and a vertical integral scale of 4.3 m. Plots of the experimental semivariograms as well as the fitted function in the two directions are given in Figure 3. The experimental semivariogram in the vertical direction suggest non-stationarity, as no sill is reached. Unfortunately, there are no tractable stochastic upscaling methods that can handle trends in core scale logconductivity, so we decided to go ahead based on the *model decision* that the core scale logconductivities constitute a stationary random field.

Above statistics are sufficient to calculate the horizontal and vertical block conductivity of rectangular blocks with the upscaling method of Indelman and Dagan [19,20]. For a step by step description of the upscaling procedure one is referred to Bierkens [2]. As representative conductivities were sought for the entire upper sublayer the block conductivities were calculated for a block of size $750 \times 750 \times 2.8$ m, where 750×750 m are the horizontal dimensions of the research area and 2.8 m the average depth of the upper sublayer. The upscaling procedure resulted in a mean horizontal block conductivity of 0.00438 m/d (with 95% confidence interval of 0.00369, 0.00519 m/d) and a mean vertical block conductivity of 0.00254 m/d (with 95% confidence interval of 0.00214, 0.00298 m/d). The C-value follows from the ratio of the average thickness (2.8 m) and the mean vertical block conductivity. This yielded a mean C-value of 1111 days with a 95% confidence interval of 914, 1313 days. This shows that the C-value that followed from the upscaling of Indelman and Dagan [19,20] did not significantly differ from the C-value obtained from the traditional method. This is not surprising, because in horizontally layered sediments and (on average) vertical head gradients we can expect almost strictly vertical flow.

Case 2: Modelling groundwater flow through a complex confining layer

Confining layers with a simple architecture such as the Purmerbos case are rare. More often they have a very complex architecture, especially in the Western Fluvial

(A)



(B)

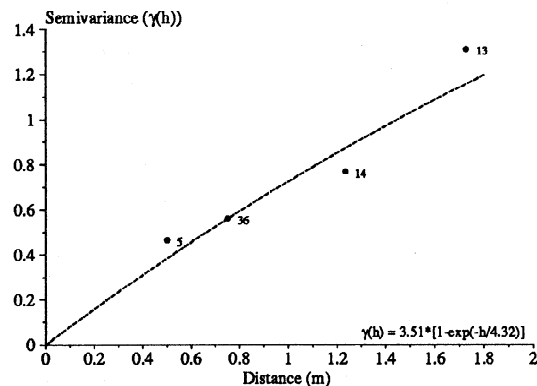


Figure 3. Semivariograms of logconductivity at the core scale; A) horizontal direction; B) vertical direction (number are number of sample pairs per lag).

District of the Netherlands. To analyze the protective properties of these complex confining layers it is not sufficient to partition them into sublayers of predominantly horizontal and vertical flow. Instead the local scale problem has to be solved in three dimensions in very fine detail. This implies that numerical groundwater models must be used with very small blocks or elements: vertical dimension of a few metres and horizontal dimensions of not more than 100 m. Pumping tests are usually too large to obtain representative parameters for these model blocks or elements. They must therefore be obtained from upscaling of conductivity measurements on sediment cores. This means that the upscaling problem plays a central role when modelling the local scale groundwater flow through complex confining layers.

The goal of the case study performed in the Schelluinen study area (Figure 6) was to test the practical feasibility and necessity of upscaling methods in local scale groundwater problems [2]. In other words, to investigate whether it is indeed possible to obtain the representative conductivities for all the blocks of a numerical model of a heterogeneous porous medium and to verify if it is indeed necessary to upscale the hydraulic conductivity from core scale measurements to model blocks.

Figure 4 shows a surficial geological map of the Schelluinen area. It also shows the location of two geological cross-sections of the confining layer that were taken by drilling 110 boreholes at 20 m intervals and sampling the texture of the sediments every 10 cm. Figure 5 shows the interpreted cross-sections.

These cross-sections show that the architecture of the confining layer is indeed very complex. The subsoil, which forms the upper aquifer, consists of eolian and fluvial deposits from the last ice-age. The confining layer itself is built up of deposits of three river systems alternated by layers of peat. To model the local scale groundwater flow through these deposits one needs a three-dimensional numerical groundwater model with small model blocks. In this case we used model blocks of $20 \times 20 \times 0.5$ m.

To infer a three-dimensional model of block hydraulic conductivities of the confining layer the following steps were taken:

- 1) classify the borehole data to appropriate texture classes that can be easily identified in the field;
- 2) take, for each texture class, undisturbed core samples and use laboratory measurements to determine the multivariate Gaussian distributions of logconductivity at the core scale;
- 3) use geological maps and the classified texture class data at the borehole sites to simulate three-dimensional stochastic images of texture classes at the model block scale. Model blocks of $20 \times 20 \times 0.5$ m are used. A model block is thought to consist of a single texture class. The stochastic images are obtained by means of conditional multiple indicator simulation;
- 4) use the statistical upscaling method of Indelman and Dagan [19,20] to derive the statistics of the multivariate distribution of the hydraulic conductivity tensors at the model block scale from the multivariate distribution at the core scale. This is

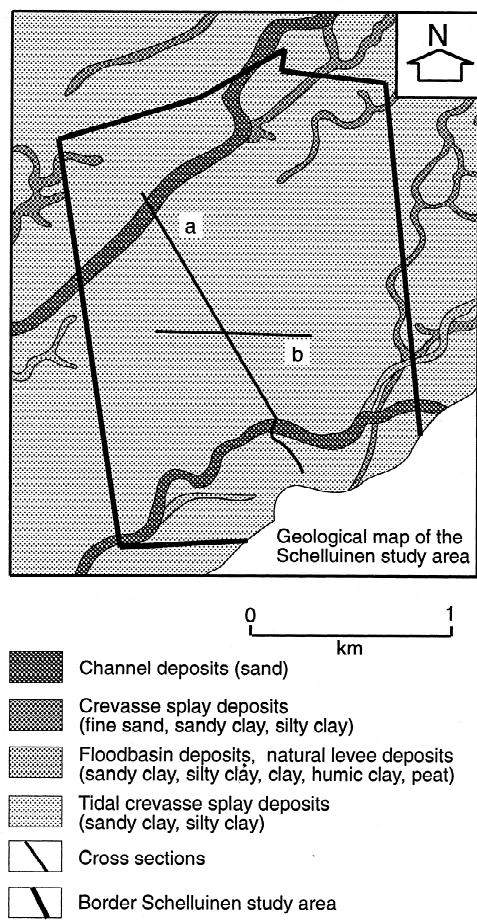


Figure 4. A map of superficial geology of the Schelluinen study area; the lines marked (a) and (b) are cross-sections referred to in the text (adapted from Weerts and Bierkens, 1993).

done separately for each texture class. The log-conductivity tensor at the model block scale is approximately Gaussian distributed [18];

- 5) use a multivariate Gaussian approach to *directly* simulate block conductivity tensors with the parameters resulting from the Indelman and Dagan upscaling approach. Again this is done separately for each texture class;
- 6) assemble the block model of the confining layer by assigning to each block a block conductivity tensor from the particular simulated field corresponding to its simulated texture class.

Once the block model of the confining layer was inferred we used the results of step 6 together with a numerical groundwater model to derive the groundwater heads and fluxes at the local scale and representative hydraulic properties at the regional scale.

We will not describe these steps in detail as they are described extensively in Bierkens [2,3]. Instead, the most important results of the various steps are summarized.

Steps 1 and 2

A total of 313 undisturbed samples were taken from different types of sediments in the study area and in two additional areas in the fluvial district. Samples from sandy sediments were 30 cm long and had a diameter of 7 cm. Samples from clayey and peaty sediments were 5 cm long with a diameter of 5 cm. The 313 samples were assigned to eight so called 'texture classes' which were distinguished on the basis of differences in geogenesis, lithology and organic matter content. Hydraulic conductivity of the samples was measured using a permeameter [2,39]. For each texture class the natural logarithm of the core scale hydraulic conductivity was assumed to be a scalar and modelled as a stationary multivariate Gaussian random field with equal integral scales in the horizontal direction and a different (smaller) integral scale in the vertical direction. In the same way as described for the first case study, the statistics of the random fields of each of the texture classes were estimated from histograms and estimated variograms. Table 1 gives a summary of all of the statistics that were inferred (or assumed) for the core scale conductivities of each texture class.

Step 3

In the Schelluinen study area a total of 229 drillings were made (110 of these in the cross-sections of Figure 5). Texture classes were determined for every 10 cm but generalized to depth intervals of 50 cm. A 50 cm interval of a drilling was assumed to be representative for a $20 \times 20 \times 0.5$ m block around it. Using a technique called 'indicator simulation' [16,22] stochastic images (realizations) were generated of the three-dimensional texture class distribution of the confining layer at the scale of the model blocks (see Bierkens and Weerts [4] for an elaborate description of the simulation method). The simulation procedure is such that the stochastic images reflect the texture classes found at the drilling sites as well as the probability of texture class occurrence and the spatial connectivity properties of the texture classes. Figure 6 shows the results for one realization. Figures 6A and 6B show the same cross-sections as Figure 5, while Figure 6C shows a horizontal cut of the realization at a depth of 2.5 m below the surface.

Table 1. Statistics of multivariate probability distribution functions of core scale $\ln(k)$; values between brackets are assumed; N number of samples, $E[\cdot]$ statistical expectation, σ variance, I_{yh} and I_{yv} horizontal and vertical integral scale; (k in md^{-1}).

Class	N	$E[\ln(k)]$	σ_y^2	I_{yh} (m)	I_{yv} (m)
1) Fluvial medium to coarse sand	118	2.741	0.660	6.25	3.75
2) Eolian medium to coarse sand	35	2.751	0.0638	1.00	0.35
3) Fine and loamy sand	8	0.603	1.756	(0.70) ^{a)}	(0.10) ^{a)}
4) Sandy to silty clay	23	-4.973	3.490	0.70	0.10
5) Clay and humic clay	40	-6.625	2.496	0.30	0.10
6) Peat	19	-1.991	1.701	0.10	(0.10) ^{b)}
7) Compacted peat	27	-4.100	2.177	0.15	0.10 ^{c)}
8) Unsaturated samples ^{d)}	43	-4.793	7.735	~	~

^{a)} Assumed the same values as for sandy to silty clay (class 4)

^{b)} Assumed the same as for the class compacted peat

^{c)} Sill reached within 0.10 meter (sample length) and set to 0.10 m

^{d)} Assumed to be a pure nugget process $K_{eff} = e^{-4.793} (1 + 7.735/6) = 0.0190 \text{ md}^{-1}$

Step 4

With the statistical parameters of the random fields of core scale hydraulic conductivities (Table 1) the statistical parameters of the random fields of block scale hydraulic conductivities can be derived with the upscaling method of Indelman and Dagan [19,20]. This was done separately for each texture class for blocks of $20 \times 20 \times 0.5$ m. The statistics of the block scale random fields are given in Table 2. We see that, although the core scale hydraulic conductivities were assumed scalar their anisotropic spatial covariance structure resulted in different mean block conductivities in the horizontal and in the vertical directions.

Steps 5 and 6

A single realization of block conductivities for the confining layer is now built by first simulating a realization of block conductivity tensors for each texture class separately (assuming multivariate logGaussian block conductivities and using the statistics of Table 2) and then combine these with a realization of texture classes (from step 3). This is achieved by assigning to each block a block conductivity tensor from the particular simulated field corresponding to its simulated texture class.

One of the realizations of block conductivities was used as input for a steady state numerical groundwater model (modelcode by McDonald and Harbaugh [20]). The groundwater model was calibrated to the natural flow situation by adjustment of the areal groundwater recharge and the drainage resistance of the water courses. For the calibration the yearly averaged heads of 12 piezometers (monitoring screens at various depths) were used. With the calibrated groundwater model the head distribution of confining layer and fluxes through the confining layer were calculated for the situation with a pumping well just north of the study area. By dividing the average difference between the groundwater table and the hydraulic head in the aquifer by the total flux through the confining layer we obtained an estimate of the C-value of the entire confining layer in the study area (this a regional scale hydraulic property). This resulted in a C-value of 1350 days. A second realization of block scale hydraulic conductivities yielded a C-value of 1310 days. These results were compared to the C-values obtained from three pumping tests that were performed at three different locations in a similar area twenty kilometres north of the study area [35]. These C-values were: test 1: 1400–1700 days; test 2: 800–1200 days; test 3: 1600–1900 days. It shows

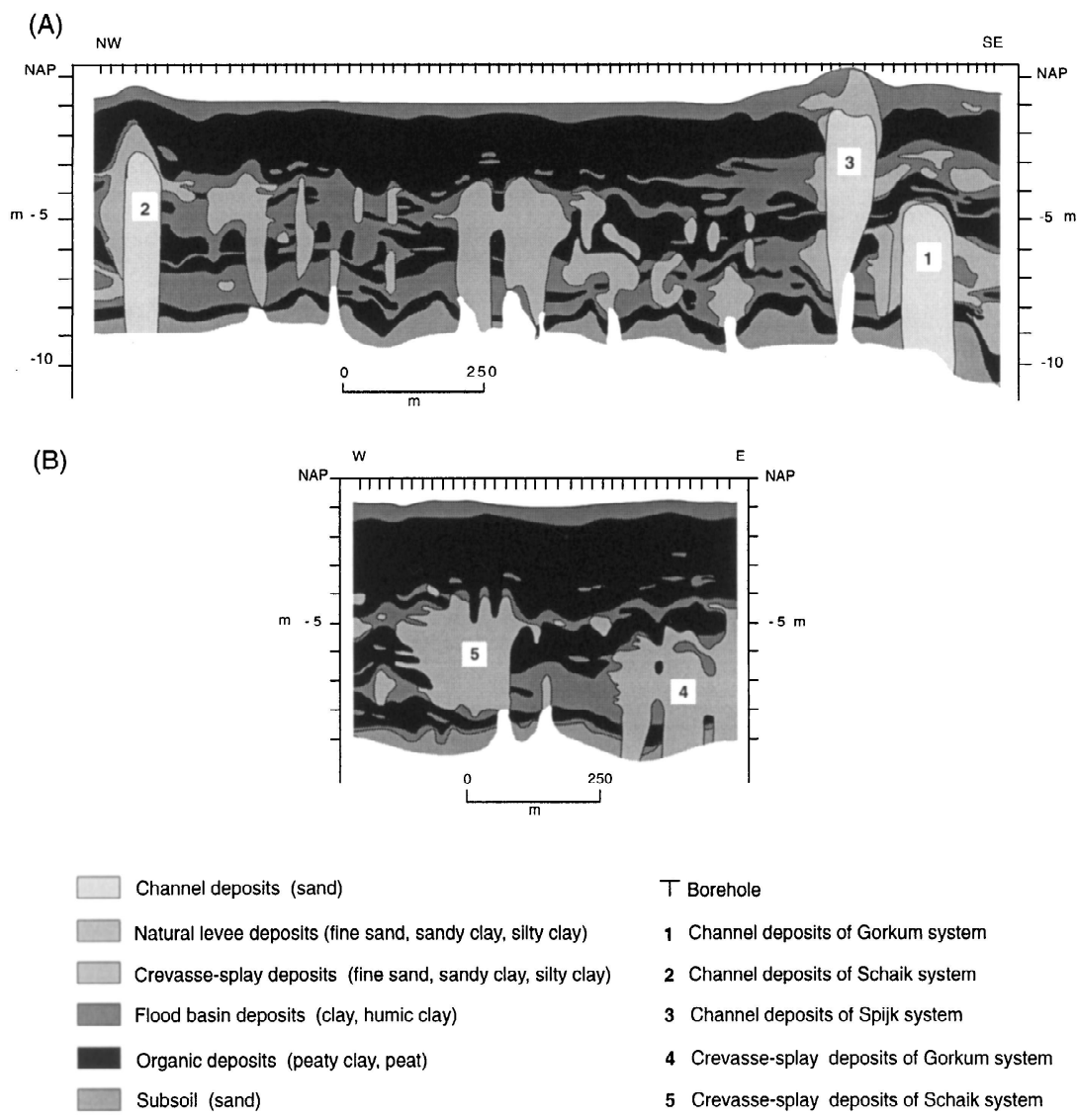


Figure 5. Cross-sections showing the deposits of the confining layer in the Schelluinen study area; A) (a) in Figure 4; B) (b) in Figure 4 (adapted from Weerts and Bierkens, 1993).

that these pumping test results were nicely compatible with the modelling results. Although it was impossible to validate the upscaling itself, at least the resulting regional scale hydraulic resistance was in accordance with that obtained from pumping tests.

Another regional scale property that is important for groundwater protection is the travel time distribution. For a net infiltration case, we can derive from this distribution the probability that a dissolved pollutant, released anywhere in a ditch or near the phreatic surface, takes a certain time to reach the underlying

aquifer, of course only taking account of advection and disregarding dispersion and diffusion. The travel time distribution of flow through the confining layer is therefore 'a time to disaster' distribution. After assigning effective porosities to the model blocks, we can calculate the travel time distribution with a particle track program [29]. The effective porosity, defined as the volume fraction water that contributes to the groundwater flow, was also measured on the 313 samples for each texture class [2]. Figure 7A shows on a logarithmic scale the travel time distributions as calculated

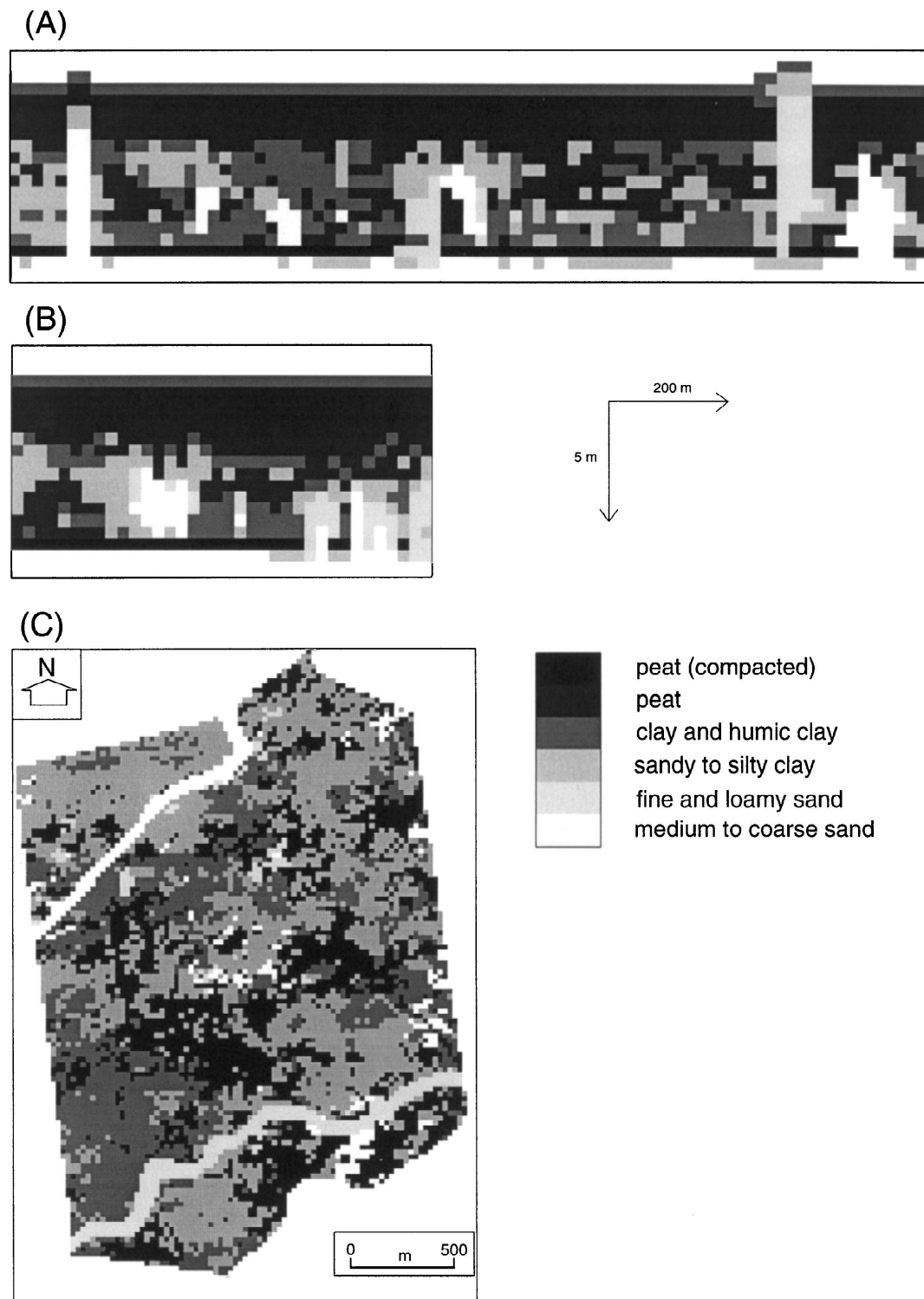


Figure 6. Realization of texture classes for the Schelluinen study area; A) cross-section (a) of Figure 4; B) cross-section (b) of Figure 4; C) horizontal cut at 5 m below the surface.

Table 2. Multivariate distribution statistics of hydraulic properties at the block scale (K_B in md^{-1}).

Class	$E[\ln(K_{bh})]$	$E[\ln(K_{bv})]$	$\sigma_{Y_b}^2$	I_{Ybh} (m)	I_{Ybv} (m)
1) Fluvial medium to coarse sand	2.840	2.770	0.166	15.26	6.24
2) Eolian medium to coarse sand	2.770	2.743	0.000791	10.69	0.76
3) Fine and loamy sand	1.136	-0.175	0.00685	10.51	0.35
4) Sandy to silty clay	-4.099	-6.440	0.0136	10.51	0.35
5) Clay and humic clay	-6.042	-7.037	0.00200	10.10	0.35
6) Peat	-1.741	-1.741	0.000340	7.22	0.40
7) Compacted peat	-3.704	-3.990	0.000435	9.00	0.35

with the groundwater model and the particle track program for the two realizations of block hydraulic properties. As can be seen travels times varied enormously; between 310 days and 50000 years. It should be noted that the effective porosities of the clayey samples were only approximate, so that the maximum travel times may well be smaller or larger by a factor 2.

An important question is whether all the effort involved in upscaling the core scale hydraulic conductivities to hydraulic conductivities at the block scale is necessary to obtain an accurate representation of the local groundwater flow and the regional scale hydraulic properties. We tested this by assigning to the model blocks of the first realization for each texture class the scalar hydraulic conductivity $K_g(1 + \sigma_y^2/6)$ as calculated from the multivariate distributions at the core scale (Table 1). This expression gives the small perturbation form of the effective conductivity for Gaussian and isotropic $y=\ln(k)$ and uniform flow [17]. When the model was run with these conductivities, while all other parameters remained the same, a C-value of 320 days was obtained! This is clearly much smaller than the C-value of the original model (1350 days) and not at all comparable to the pumping test results performed north of the study area [35]. In Figure 7B the travel time distribution is given for this run. On average, the travel times were underestimated. Clearly, upscaling of core scale hydraulic conductivities to model block scale hydraulic conductivities, or obtaining block conductivities in some other manner, was necessary to obtain meaningful results. This is a general result for these types of deposits. The combination

of a large variance and a large statistical anisotropy of core scale hydraulic conductivities of the texture classes fine sand and loamy sand and sandy to silty clay, which is caused by an alternation of thin horizontal layers of very different conductivity in these sediments, results in small vertical hydraulic conductivities at the model block scale. These in turn result in a larger C-value and larger travel times.

Conclusions

This paper has shown that particularly for the modelling of local scale groundwater flow in heterogeneous formations the upscaling of hydraulic conductivities is a crucial step. One could make a similar case for the modelling of advective and dispersive transport [33] or unsaturated flow [13,31].

Upscaling of hydraulic conductivity should be such that the calculated mass transfer (e.g fluxes) and change of momentum (e.g. head gradient) are the same at the smaller and the larger scale. The result of this requirement is that block conductivities are dependent on the geometry of the groundwater flow problem, as was shown by a simple numerical example. This implies that the predictive value of calibrated models may be limited to certain flow geometries that resemble the geometry of the flow field that occurred during the calibration. This problem is probably not limited to hydraulic conductivity and groundwater flow but may occur in general when upscaling parameters of (distributed) mass-conserving models.

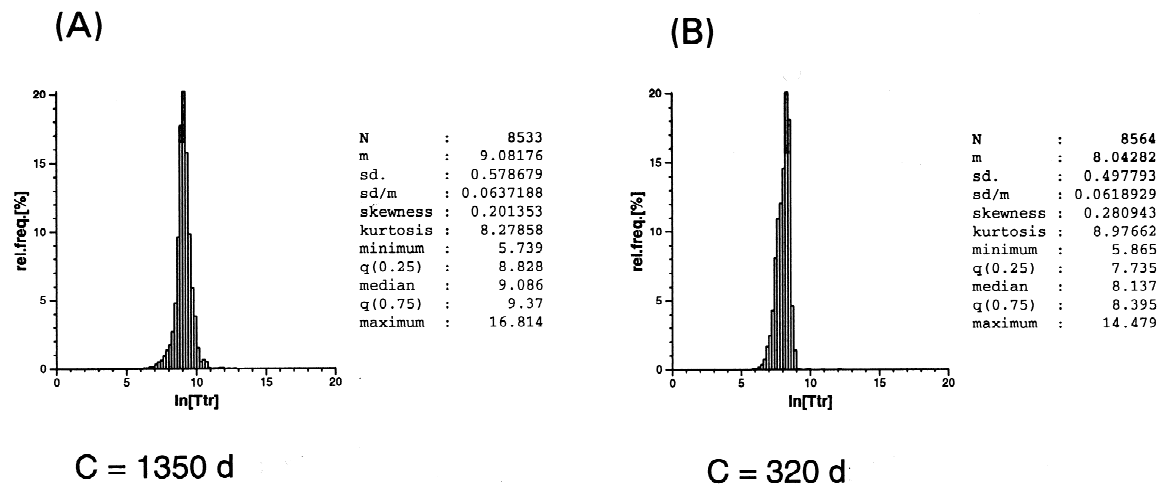


Figure 7. Travel time distributions (travel times in log(days)); A) using block conductivities; B) when core scale conductivities are used.

Analytical solutions for the upscaled hydraulic conductivity are available in both a deterministic and a stochastic setting, but only in a practical form for uniform flow. However, in practice these uniform flow solutions can give satisfactory results for non-uniform geometries, provided that the flow is slowly varying compared to the extent of the modelling domain and the model blocks.

The upscaling method of Indelman and Dagan [19,20] was applied in two case studies. The first case study showed that for horizontally layered deposits and vertical flow the upscaling method of Indelman and Dagan [19,20] yields similar results as the traditional method based on harmonic averaging. The second case study indicated that the statistical upscaling procedure of Indelman and Dagan [19,20] can be successfully applied in highly complex deposits. When the local scale groundwater flow was modelled with the upscaled block conductivities, realistic values of regional scale hydraulic properties such as C-values (hydraulic resistance) could be derived which were consistent with those obtained from pumping tests. This case study also showed that it is absolutely necessary to obtain correct estimates of block scale hydraulic conductivities when numerically modelling groundwater flow through complex deposits. If upscaling is neglected the C-value and the travel time distribution of the confining layer will be underestimated.

References

1. Bear J (1979) *Hydraulics of Groundwater*. McGraw-Hill, New-York.
2. Bierkens MFP (1994) *Complex confining layers; a stochastic analysis of hydraulic properties at various scales*. Ph.D. Thesis Utrecht University. Utrecht: Netherlands Geographical Studies 184.
3. Bierkens MFP (1996) *Modelling hydraulic conductivity of a complex confining layer at various spatial scales*. *Water Resources Research* 32(8): 2369–2382.
4. Bierkens MFP and Weerts HJT (1994) *Block hydraulic conductivity of cross-bedded fluvial sediments*. *Water Resources Research* 30(10): 2665–2678.
5. Bierkens MFP and Weerts HJT (1994) *Application of indicator simulation to modelling the lithological properties of a complex confining layer*. In: De Gruijter JJ, Webster R and Myers DE (Eds.) *Proceedings of the first international conference on Pedometrics*, Wageningen, the Netherlands. *Geoderma* 62: 265–284.
6. Carrera J and Neuman, SP (1986) *Estimation of aquifer parameters under transient and steady state conditions; 1. Maximum likelihood method incorporating prior information*. *Water Resources Research* 22(2): 199–210.
7. Dagan G (1981) *Analysis of flow through heterogeneous random aquifers by the method of embedded matrix, 1, Steady flow*. *Water Resources Research* 17(1): 107–122.
8. Dagan G (1989) *Flow and transport in porous formations*. Springer Verlag.
9. Desbarats AJ (1989) *Support effects and the spatial averaging of transport properties*. *Mathematical Geology* 21: 383–389.
10. Desbarats AJ (1991) *Spatial averaging of transmissivity*. In: Bachu (Ed.) *Proceedings of the 5th Canadian/American conference on hydrogeology: Parameter identification and estimation for aquifer and reservoir characterization*: 139–154. Dublin, Ohio: National Water Well Association.
11. Desbarats AJ (1992) *Spatial averaging of hydraulic conductivity in three-dimensional heterogeneous porous media*. *Mathematical Geology* 24(3): 249–267.

12. Desbarats AJ (1992) Spatial averaging of transmissivity in heterogeneous fields with flow toward a well. *Water Resources Research* 28(3): 757–767.
13. Desbarats AJ (1995) An interblock conductivity scheme for finite difference models of steady unsaturated flow in heterogeneous media. *Water Resources Research* 31(11): 2883–2889.
14. Forchheimer Ph (1886) Über die ergiebigkeit von brunnenanlagen und sickerschlitzen. *Zeitschrift der Architekten und Ingenieure Verein* 32: 539–563.
15. Freeze AF (1975) A stochastic-conceptual analysis of one-dimensional groundwater flow in nonuniform homogeneous media. *Water Resources Research* 11(5): 725–741.
16. Gómez-Hernández JJ and Srivastava RM (1990) ISIM3D: An ANSI-C three-dimensional multiple indicator conditional simulation program. *Computers and Geosciences* 16(4): 395–440.
17. Gutjahr AL, Gelhar L, Bakr AA and MacMillan JR (1978) Stochastic analysis of spatial variability in subsurface flows; 2. Evaluation and application. *Water Resources Research* 14(5): 953–959.
18. Indelman P (1993) Upscaling of permeability of anisotropic heterogeneous formations; 3. Applications. *Water Resources Research* 29(4): 935–943.
19. Indelman P and Dagan G (1993) Upscaling of permeability of anisotropic heterogeneous formations; 1. The general framework. *Water Resources Research* 29(4): 917–923.
20. Indelman P and Dagan G (1993) Upscaling of permeability of anisotropic heterogeneous formations; 2. General structure and small perturbation analysis. *Water Resources Research* 29(4): 925–933.
21. Journel AG and Huijbregts CJ (1978) *Mining geostatistics*. London: Academic Press.
22. Journel AG and Isaaks EH (1984) Conditional indicator simulation; Application to a Saskatchewan uranium deposit. *Mathematical Geology* 16(7): 685–718.
23. Kasap E. and Lake LW (1989) An analytical method to calculate the effective permeability tensor of a grid block and its application in an outcrop study. *SPE paper 18434*: 355–362.
24. King PR (1988) The use of renormalization for calculating effective permeability. *Transport in porous media* 4(1): 37–58.
25. Kitanides PK and Vomvoris EG (1983) A geostatistical approach to the inverse problem in groundwater modelling (steady state) and one-dimensional simulations. *Water Resources Research* 19(3): 677–690.
26. Kruseman GP and De Ridder NA (1970) *Analysis and evaluation of pumping test data*. Wageningen: ILRI Bulletin 11.
27. Matheron G (1967) *Éléments pur une théorie des milieux poreux*. Paris: Mason et Cie.
28. McDonald MG and Harbaugh AW (1988) A modular three-dimensional finite-difference ground-water flow model. In: *Techniques of water resources investigations of the USGS*. Washington DC.
29. Pollock DW (1990) MODPATH, Computer programs to compute and display pathlines using results from the U.S. Geological Survey modular three-dimensional finite-difference ground-water flow model. USGS.
30. Rubin Y and Gómez-Hernández JJ (1990) A stochastic approach to the problem of upscaling of conductivity of disordered media; Theory and unconditional simulations. *Water Resources Research* 26(4): 691–701.
31. Russo D (1992) Upscaling of hydraulic conductivity in partially saturated heterogeneous porous formation. *Water Resources Research* 28(2): 397–409.
32. Sánchez-Villa X, Girardi JP and Carrera J (1995) A synthesis of approaches to upscaling of hydraulic conductivities. *Water Resources Research* 31(4): 867–882.
33. Scheibe TD and Cole CR (1994) Non-Gaussian particle tracking; Application to scaling of transport processes in heterogeneous porous media. *Water Resources Research* 30(7), 1994.
34. Sudicky EA (1986) A natural-gradient experiment on solute transport in a sand aquifer; Spatial variability of hydraulic conductivity and its role in the dispersion process. *Water Resources Research* 22(13): 2069–2082.
35. Timmerman PHA and Hemker CJ (1993) Bepaling van de intreeweerstand van de Lek en de verticale weerstanden van de uiterwaarden en polders nabij Langerak (Alblasserwaard). *H₂O* 26(1): 2–7.
36. Van der Gaast JWJ and Peerboom JPM (1996) *Geohydrologisch veldonderzoek Purmerbos; Uitwerking en interpretatie van doorlatendheidsmetingen en twee pompproeven in het Purmerbos*. Wageningen: DLO-Staring Centrum, rapport 437.
37. Weerts HJT and MFP Bierkens (1993) Geostatistical analysis of overbank deposits of anastomosing and meandering fluvial systems; Rhine-Meuse delta, the Netherlands. In: Fielding CR (ed.) *Proceedings of the 5th International Congress on Fluvial Sedimentology*. *Sedimentary Geology* 85: 221–232.
38. Whitaker S (1996) *Transport phenomena in porous media; The method of volume averaging* (in press).
39. Wit KE (1963) *Apparatuur voor het meten van de doorlatendheid in ongestoorde monsters*. Wageningen: ICW rapport 17.
40. Zijl W and Stam JMT (1992) Modelling permeability in imperfectly layered porous media; I. Derivation of block-scale permeability tensor for thin grid-blocks. *Mathematical Geology* 24(8): 865–883.